

Nuclear-Spin Waves in Polarized Atomic Hydrogen Gas: Temperature and Density Dependence in the Hydrodynamic and Knudsen Regimes

N. P. Bigelow,^(a) J. H. Freed, and D. M. Lee

Laboratory of Atomic and Solid State Physics and Baker Laboratory of Chemistry,
Cornell University, Ithaca, New York 14853

(Received 19 May 1989)

Accurate measurements on the nuclear-spin waves observed in the NMR spectrum of spin-polarized atomic hydrogen provide a quantitative test of theory. Results for temperatures between 160 and 537 mK and densities between 7×10^{15} and $5 \times 10^{16} \text{ cm}^{-3}$ display the expected magnitude and $T^{-1/2}$ divergence predicted for the spin-wave quality factor μ . It is shown that spin waves persist at low enough densities (Knudsen regime) that elastic wall collisions are more probable than atom-atom exchange collisions. An anomalous increase in spin-wave widths at low temperatures is explained in terms of the enhanced effects of sticking collisions of the atoms with the walls.

PACS numbers: 67.65.+z

The transport properties of quantum gases are profoundly altered by the polarization of their constituent spins. In particular, doubly spin-polarized atomic hydrogen $^1\text{H}\downarrow$ and polarized ^3He gases,² as well as dilute mixtures³ of ^3He in ^4He , can exhibit unusual features in their NMR spectra which depend strongly on polarization. Such effects have attracted continued theoretical interest.⁴⁻⁶ They can be shown to result from the effects of quantum indistinguishability during interatomic collisions, even though these systems are not degenerate. In $\text{H}\downarrow$, the NMR spectrum is marked by a series of sharp resonances due to standing spin-wave modes¹ as shown in Fig. 1, representing significant quantum corrections to this otherwise ideal gas.

In this Letter we report on the first quantitative measurement of the temperature dependence of μ , the quality factor for the nuclear-spin waves observed in the NMR spectrum of $\text{H}\downarrow$ in the hydrodynamic regime, and this demonstrates that μ diverges as $T \rightarrow 0$. We also describe spin waves observed at low densities, which provide a novel example of quantum behavior in an otherwise simple Knudsen gas, implying that even as the density $n \rightarrow 0$ spin waves can persist.

Spin waves in rarefied spin-polarized gases with a broken symmetry are predicted⁴⁻⁶ when the thermal wavelength (λ_T) is long compared to the range of the interparticle potential (given by the s -wave scattering length $a_s = 0.72 \text{ \AA}$). These theories describe transport in the hydrodynamic limit in terms of coupled nonlinear differential equations for the spin current and density. For the case of NMR experiments with small tipping angle (so $M_+ \ll M_z \approx |M|$), the equations can be linearized, and in a rotating frame, one has

$$i \frac{\partial M_+}{\partial t} = \{\gamma \delta H_0 + i D_0 [(1 + i\mu P)/(1 + \mu^2 P^2)] \nabla^2\} M_+, \quad (1)$$

where $M_+ = M_+(r, t) = M_x + iM_y$ is the complex transverse spin density and γ is the effective nuclear gyromagnetic moment. D_0 is the self-diffusion coefficient, which

is independent of the nuclear polarization, $P = (n_a - n_b)/(n_a + n_b)$, where n_a and n_b are the populations of the lower two hyperfine states. δH_0 results from the residual gradient in the static magnetic field $\mathbf{H}(r) = H_0(r)\hat{z}$. The quality factor μ is a direct measure of the relative importance of spin-rotating exchange collisions in comparison to diffusive momentum-changing collisions. At low temperatures, μ reflects just the temperature dependence of exchange (i.e., $|\mu| \approx \lambda_T/a_s$). The form of Eq. (1) is that of a "Schrödinger equation with damping" in which the "potential" involves the static field gradient and the

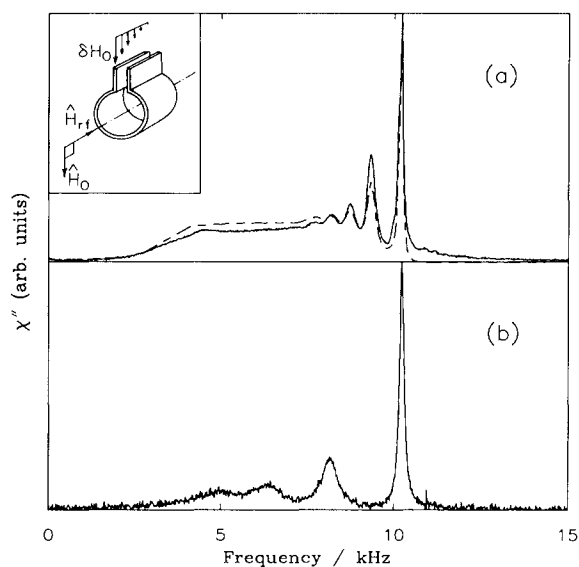


FIG. 1. Spin-wave spectra in (a) hydrodynamic ($n = 4 \times 10^{16} \text{ cm}^{-3}$) and (b) Knudsen ($n = 1 \times 10^{14} \text{ cm}^{-3}$) regimes. Here $T = 373 \text{ mK}$ and $G = 1.7 \text{ G/cm}$. Spectra are scaled for comparison. The dashed line in (a) is the best fit to the simulation based on hydrodynamic model; in (b) it is not properly fit by the hydrodynamic model. Inset: Arrangement of resonator, static field H_0 , gradient δH_0 , and rf field H_1 .

“kinetic energy” involves an effective complex diffusion coefficient.

Consider the case of a *linear* field gradient along the \hat{x} direction ($\delta H_0 = Gx$). The solutions to Eq. (1) depend upon the applied boundary conditions (BC). We usually employ “reflecting-wall” BC’s which correspond to negligible spin relaxation at the walls (i.e., $\mathbf{J} \cdot \hat{n} = 0$, where \hat{n} is the normal to the surface). The spin-wave modes are the “stationary-state” solutions to Eq. (1). They are just Airy functions when the modes are confined both by the appropriate cell wall and by the magnetic field gradient.^{7,8} The complex eigenvalues are

$$\bar{\omega}_m = -a_m \{ (\gamma \delta H_0)^2 D_0 (i + \mu P) / (1 + \mu^2 P^2) \}^{1/3}, \quad (2)$$

where m is the mode index and a_m is found from the zero of the derivative of the m th Airy function Ai . This gives the dispersion relations for these modes. The real part $\text{Re}[\bar{\omega}_m] = \omega_m$ is the frequency of the mode relative to the Larmor frequency at the reflecting boundary, while the imaginary part $\text{Im}[\bar{\omega}_m] \equiv \Gamma_m$ is the width of that mode.

We determined μ and D_0 through a careful analysis of the spin-wave spectra. The apparatus is similar to that described in earlier work¹ but with modifications to greatly improve the field homogeneity and the control of the field gradient. The present configuration has a minimum gradient of 0.1 G/cm at $H_0 = 7.13$ T. Most of the experiments were performed using a linear static magnetic field gradient of 1.7 or 2.1 G/cm along the long ($L = 1.025$ cm) axis of the cylindrical loop-gap¹ NMR resonator (tuned for 1.021 GHz) as shown in the inset of Fig. 1. These gradients were chosen to produce a series of well-defined spin-wave modes without creating an excessively fast free induction decay (FID) of the diffusive modes. The broad background line shape observed in the spectrum can be described in terms of the diffusive spin-wave modes.^{7,8} In the Schrödinger analogy, our choice of gradient means that the potential term is large compared with the kinetic term, so that a fair number of spin-wave modes are well confined.

The measurements were made using a heterodyne NMR spectrometer with quadrature detection and with minimum sensitivity of $\approx 2 \times 10^{13}$ polarized spins. Temperatures were calibrated against the ^3He melting curve and pressures were measured using a capacitive strain gauge of minimum resolution $6.7 \times 10^{13}/T$ (cm^{-3}/K). The strain gauge was calibrated against the ^4He vapor-pressure scale. To estimate sample densities near or below the strain gauge resolution, the NMR signal was used. The magnetization as measured by the initial FID amplitude (for which the polarization P is known, cf. below) was first calibrated against the density measured by the strain gauge in the high-density regime ($n > 10^{15} \text{ cm}^{-3}$). The relation was found to be linear and temperature independent over the region of interest and was extrapolated to determine the low densities.

Experiments were initiated by loading a sample of atomic hydrogen to a high density ($\approx 10^{17} \text{ cm}^{-3}$). The sample was allowed to achieve high nuclear polarization through preferential recombination.^{9,10} Experiments were performed by maintaining the cell at a given temperature and applying small ($\approx 7^\circ$) tipping pulses. The NMR FID’s were digitized and stored for analysis. Surface recombination limited the maximum density at the lowest temperatures to $2 \times 10^{15} \text{ cm}^{-3}$. To minimize the effects of surface recombination due to one-body relaxation and to assure the highest possible nuclear polarizations, a layer of solid H_2 was preplated onto the cell walls¹¹ before the start of each run. All experiments were performed with saturated superfluid- ^4He coatings on the cell walls.

The FID’s were initially fit to a set of damped exponentials (Lorentzians) using a linear prediction^{12,13} which provides accurate amplitudes, frequencies, and widths. Then the frequencies and widths of the four most prominent peaks were simultaneously fit by Eq. (2) using a nonlinear least-squares minimization yielding μ and D_0 . The value of the field gradient is obtained from fitting the inhomogeneously broadened background line shape [cf. Fig. 1(a)]. However, Eq. (2) neglects any perturbation of the modes by the reflecting cell wall at the field maximum. To account for this perturbation, the Fourier transform (FT) of the FID was then fit to a numerical solution^{5,8} of Eq. (1), also by least-squares minimization using the results of the first analysis as seed values. At the higher temperatures and densities the modes were found to adhere remarkably well to Eq. (2). At lower densities and temperatures, deviations

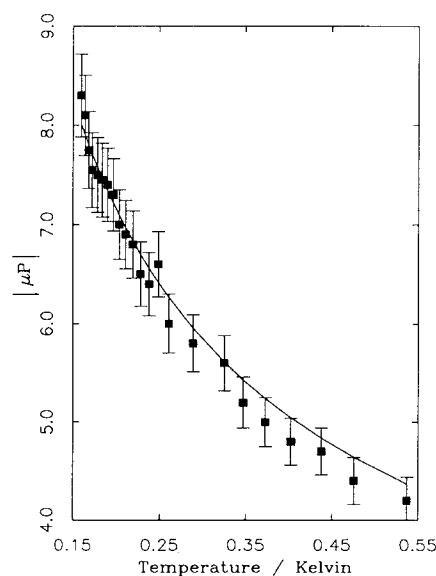


FIG. 2. Plot of $|\mu P|$ vs temperature for densities n between 7×10^{15} and $5 \times 10^{16} \text{ cm}^{-3}$. The solid line is the best fit to predicted $T^{-1/2}$ limiting dependence (as $T \rightarrow 0$).

were observed, especially for the higher modes (cf. the error bars in Fig. 2).

Results for μ are shown in Fig. 2. Note that for $H\downarrow$, μ is negative¹ and we observe it diverging as $T \rightarrow 0$. The solid line is a best fit to the predicted temperature dependence of $T^{-1/2}$ which yields a value of 3.2 ± 0.25 for $|\mu P T^{1/2}|$. Since $|P| \leq 1$ this result immediately gives a lower bound to $|\mu T^{1/2}|$. From recombination experiments we find the sample polarization to be 0.9 ± 0.1 yielding a value of 3.5 ± 0.4 for $|\mu T^{1/2}|$ to be compared with the theoretical value^{5,14} of 3.65. Our results are also characterized by $nD_0 = 1.3 \times 10^{18} \text{ cm}^{-1} \text{ sec}^{-1}$ to be compared to the prediction^{5,14} of $1.5 \times 10^{18} \text{ cm}^{-1} \text{ sec}^{-1}$. As expected, for $H\downarrow$ gas⁴ in the hydrodynamic regime, nD_0 is density and temperature independent over the experimental range.^{5,14}

As the temperature is decreased from 537 to 200 mK, the mode width decreases monotonically as shown in Fig. 3. This mode narrowing [consistent with Eq. (2)] is due to the increase in $|\mu|$ as λ_T increases. However, as the sample is cooled below 200 mK, the linewidths increase dramatically. When corrected for density, the splittings between spin-wave modes do *not* show a similar deviation in temperature dependence compared to their behavior at higher temperatures and densities. This observation cannot be attributed to a change in the reflecting BC's used to solve Eq. (1) (provided they remain spin independent) or to ^4He atoms in the gas.

To describe this result we introduce an additional broadening term Γ' to the width of each mode Γ_n . This term represents dephasing effects due to the small change in the contact hyperfine interaction (hence a change Δ in the Larmor frequency) when $H\downarrow$ atoms stick to the cell wall. To estimate Γ' we treat the effect of surface dephasing in a manner similar to Jochemsen *et al.*¹⁵ Γ' depends on the mean sticking time τ_s and Δ . The sticking coefficient s is used to relate τ_s to the time be-

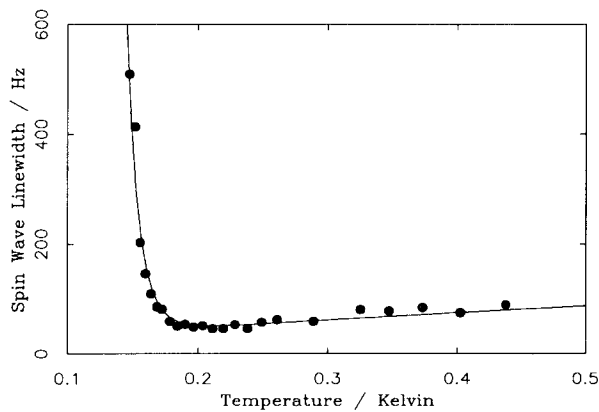


FIG. 3. Linewidth Γ_1 of first spin-wave mode vs temperature. The solid line is that predicted using the measured values of μP and D_0 . Below 200 mK the solid line also reflects the best fit to Γ' (cf. text).

tween sticking events τ_b . We also require the binding energy E_b and the area-to-volume ratio of the cell. The measured values of $E_b = 1.05 \pm 0.02 \text{ K}$,^{9,10} $s = s(T) = 0.33T$ (T in K),^{16,17} and $\Delta = 23.0 \text{ kHz}$ (Refs. 15 and 17) were used giving $\Gamma' = 2.3 \times 10^{-6} T^{-5/2} \exp(2E_b/k_B T)$. Results of a fit with the mode width using $\Gamma' = CT^{-5/2} \exp(2E_b/k_B T)$ yielded $C = (2.6 \pm 0.3) \times 10^{-6}$. We have not pursued this fit as an accurate measurement of sticking coefficient or the wall shift, because these quantities occur as a product, and there remain some questions of model dependence.^{18,19}

Perhaps most surprising is the observation of well-defined spin-wave modes in the NMR spectrum at densities below 10^{14} cm^{-3} . The spectra at these densities are to be distinguished from the higher-density hydrodynamic results by the absence of any inhomogeneously broadened background line shape [cf. Fig. 1(b)]. Its absence is due to motional averaging of the static field gradient which occurs as the atoms traverse the sample cell relatively unhindered by gas-phase collisions. To appreciate the nature of the spin waves in this density regime, consider the gas density and temperature of Fig. 1(b), 10^{14} cm^{-3} at 373 mK. Relevant mean free paths are for s -wave scattering $l_a \approx 43 \text{ cm}$, for the thermally averaged diffusive scattering¹⁴ $l_d \approx 4.4 \text{ cm}$, and for forward exchange scattering, the dominant term for spin rotation,¹⁴ $l_{\tau_{\text{rad}}} \approx 1.1 \text{ cm}$. A comparison between these mean free paths and the sample size L suggests a breakdown in the hydrodynamic limit. A more precise criterion²⁰ for the hydrodynamic limit is $L^2/D_0 > l_d/\langle v_T \rangle$, where $\langle v_T \rangle$ is the mean thermal velocity. For Fig. 1(b), L^2/D_0 and $l_d/\langle v_T \rangle$ are, respectively, 81 and 513 μsec . However, nonsticking collisions with the cell walls are essentially elastic at these temperatures,¹⁸ and above 200 mK we find (cf. above) that we can treat the wall collisions as reflecting. In the absence of spin-dependent wall effects, the spin state of a reflecting atom can remain coherent with the other atoms in the sample even when wall collisions are as frequent as interparticle collisions. Only spin-dependent inelastic scattering processes disrupt the coherence of the spin-wave function. Thus spin waves can persist even as $n \rightarrow 0$.²¹ In contrast, at temperatures below 200 mK the spin-wave spectrum begins to wash out as sticking wall collisions disrupt the coherence of the atomic spins.

The sensitivity of the spin-wave mode widths to surface sticking indicates that spin-wave spectroscopy could provide a tool for detecting the onset of the expected²² quantum reflection in $H\downarrow$. As the temperature decreases, the boundaries are predicted to become more reflective and this would decrease the observed widths. It would also reduce the thermal accommodation with the cell walls. By studying the spin-wave spectrum at various field gradients, the surface effects can be isolated, and it should be possible to measure the temperature of the gas via μ .

We would like to thank Bryan Statt for invaluable as-

sistance in this work. This work was supported by NSF Grant No. DMR-8616727.

^(a)Present address: AT&T Bell Laboratories, Holmdel, NJ 07733.

¹B. R. Johnson, J. S. Denker, N. Bigelow, L. P. Lévy, J. H. Freed, and D. M. Lee, *Phys. Rev. Lett.* **52**, 1508 (1984).

²P. J. Nacher, G. Tastevin, M. Leduc, and F. Laloë, *J. Phys. (Paris) Lett.* **45**, L411 (1984).

³W. J. Gully and W. J. Mullin, *Phys. Rev. Lett.* **52**, 1810 (1984).

⁴C. Lhuillier and F. Laloë, *J. Phys. (Paris)* **43**, 197 (1982); **43**, 225 (1982).

⁵L. P. Lévy and A. E. Ruckenstein, *Phys. Rev. Lett.* **52**, 1512 (1984).

⁶E. P. Bashkin, *Pis'ma Zh. Eksp. Teor. Fiz.* **33**, 11 (1981) [*JETP Lett.* **33**, 8 (1981)].

⁷J. H. Freed, *Ann. Phys. (Paris)* **10**, 901 (1985).

⁸N. P. Bigelow, Ph.D. dissertation, Cornell University, 1989 (unpublished).

⁹I. F. Silvera and J. T. M. Walraven, in *Progress in Low Temperature Physics*, edited by D. F. Brewer (North-Holland, Amsterdam, 1986), Vol. 9, p. 139.

¹⁰T. J. Greytak and D. Kleppner, in *New Trends in Atomic Physics*, Proceedings of the Les Houches Summer School, Session XXXVIII, edited by G. Grynberg and R. Stora (North-Holland, Amsterdam, 1984).

¹¹B. W. Statt, A. J. Berlinsky, and W. N. Hardy, *Phys. Rev. B* **31**, 3169 (1985).

¹²H. Barkhuijsen, R. de Beer, W. M. M. J. Bovée, and D. van Ormondt, *J. Magn. Reson.* **61**, 465 (1985).

¹³N. P. Bigelow, J. H. Freed, D. M. Lee, and B. W. Statt, in *Spin Polarized Quantum Systems*, edited by S. Stringari (World Scientific, Teaneck, NJ, 1989), p. 231.

¹⁴C. Lhuillier, *J. Phys. (Paris)* **44**, 1 (1983).

¹⁵R. Jochemsen, M. Morrow, A. J. Berlinsky, and W. N. Hardy, *Phys. Rev. Lett.* **47**, 852 (1981).

¹⁶J. J. Berkhout, E. J. Wolters, R. van Roijen, and J. T. M. Walraven, *Phys. Rev. Lett.* **57**, 2387 (1986).

¹⁷L. Pollack, Ph.D. dissertation, MIT, 1989 (unpublished); (private communication).

¹⁸J. J. Berkhout and J. T. M. Walraven, in *Spin Polarized Quantum Systems*, edited by S. Stringari (World Scientific, Teaneck, NJ, 1989), p. 201.

¹⁹Note that the frequency shift from this mechanism (Ref. 15) affects all spin-wave modes identically and thus does *not* affect their splitting.

²⁰J. P. Bouchaud, Ph.D. dissertation, Université de Paris, 1985 (unpublished); J. P. Bouchaud and C. Lhuillier, *J. Phys. (Paris)* **46**, 1135 (1985).

²¹E. P. Bashkin, *Usp. Fiz. Nauk* **148**, 433 (1986) [*Sov. Phys. Usp.* **29**, 238 (1986)]; A. E. Meyerovich, in *Progress in Low Temperature Physics*, edited by D. F. Brewer (North-Holland, Amsterdam, 1987), Vol. 11, p. 1.

²²Y. Kagan and G. V. Shlyapnikov, *Phys. Lett.* **95A**, 309 (1983); D. Zimmerman and A. J. Berlinsky, *Can. J. Phys.* **61**, 508 (1983).